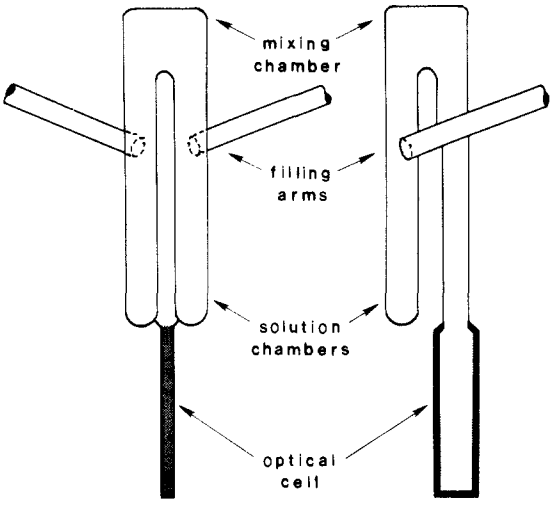


**Figure 5.** Cell used in the SCM method. The silica cuvette is joined by a graded seal to borosilicate glass.

The cell is shown in Figure 5. In a glovebox solutions of the two reactants in $SbCl_3$–$AlCl_3$–BPCl media were added by syringes into the two solution chambers and the filling arms were sealed off on a vacuum line under ~0.8 atm of purified argon. Inversion and shaking of the cell mixed the two solutions and a second inversion directed the liquid into the cuvette.

**Magnetic Resonance.** ESR experiments were carried out with a Varian Model E-109 spectrometer equipped with a Model E-257 variable temperature accessory. The temperature of the sample was controlled by means of a convective flow of heated $N_2$ and was constant to ±1 °C. The spectrometer operated at a nominal microwave frequency of 9.102 GHz, and spectra were measured with use of 100-kHz field modulation and a scan rate of ~1 G $min^{-1}$. Hyperfine coupling constants were accurate to ±0.03 G. Sample tubes and their preparation have been described.[7c] Substrate concentrations were in the range 0.1–1 mM.

$^1H$ NMR measurements were made with a Nicolet NT-200 FT spectrometer at 200.17 MHz on solutions of ~0.1 M. The chemical shifts were referenced externally to $(CH_3)_4NCl$ ($\delta$ 3.12) in molten $SbCl_3$, which was itself referenced to $(CH_3)_4Si$ in the melt. The dications of POZ and PTZ were generated chemically for NMR measurements by oxidation with an excess of $SbCl_5$ in $SbCl_3$–10 m/m $AlCl_3$.

**Acknowledgment.** We thank Dr. J. Q. Chambers for the use of his ESR spectrometer, L. L. Brown for measuring NMR spectra, and Dr. S. P. Zingg for the DM cell graphic. This research was sponsored by the Division of Chemical Sciences, Office of Basic Energy Sciences, U.S. Department of Energy under contract DE-AC05-840R21400 with Martin Marietta Energy Systems, Inc. D.M.C. was a recipient of an Atlantic-Richfield Foundation supplemental fellowship.

**Supplementary Material Available:** Figures showing spectra measured during electrolysis of POZ in 60–19–21 melt, ESR spectrum of $PTZ^{+\cdot}$ in $SbCl_3$, spectra measured during electrolysis of $PTZ^{+\cdot}$ in 60–22–18 melt, and spectra of $M(bpy)_3^{2+}$ and $M(bpy)_3^{3+}$ complexes in $SbCl_3$–$AlCl_3$–BPCl melts (5 pages). Ordering information is given on any current masthead page.

# An in Situ Infrared Spectroscopic Investigation of the Role of Ethylidyne in the Ethylene Hydrogenation Reaction on $Pd/Al_2O_3$

**Thomas P. Beebe, Jr., and John T. Yates, Jr.***

*Contribution from the Surface Science Center, Department of Chemistry, University of Pittsburgh, Pittsburgh, Pennsylvania 15260.* *Received July 16, 1985*

**Abstract:** Transmission infrared spectroscopy and kinetic techniques have been used to monitor surface ethylidyne (≥$CCH_3$) concentrations in situ during ethylene hydrogenation reactions on $Pd/Al_2O_3$ surfaces. For 1:1 mixtures of reactant $C_2H_4$ and $H_2$, there is no formation of surface ethylidyne during the ethylene hydrogenation; for reactant mixtures where $C_2H_4$ is in excess of $H_2$, the buildup of surface ethylidyne concentration with time is dependent on the amount of excess $C_2H_4$. Using $^{13}C$-labeled ethylidyne, it has been shown that ethylidyne formation and hydrogenation rates are 2 to 3 orders of magnitude slower than ethylene hydrogenation rates. Finally, ethylene hydrogenation rates have been measured on surfaces both with and without preadsorbed ethylidyne and are the same for both. This suggests that ethylidyne is a spectator species not essential to ethylene hydrogenation and that the proposed ethylidene species (on Pt(111)), proceeding from the ethylidyne species, is not a necessary species in the hydrogenation mechanism for ethylene on the typical $Pd/Al_2O_3$ catalytic surfaces employed in this study.

## I. Introduction

The catalyzed ethylene hydrogenation reaction

$$C_2H_4(g) + H_2(g) \xrightarrow{\text{catalyst}} C_2H_6(g)$$

is perhaps one of the most studied classical catalytic reactions and has been the subject of numerous reviews and papers.[1,2] Mechanisms have been proposed for this reaction as early as 1934 by Horiuti and Polanyi[3] (associative mechanism) and in 1938 by Farkas and Farkas[4] (dissociative mechanism). These basic mechanisms have been altered in many ways by various workers through the years (see ref 1 and 2). Despite this large number of studies, there is not a consensus of opinion as to the actual mechanism for $C_2H_4$ hydrogenation by the platinum group metals.

Very recently, there has been a proposal of a new mechanism in the ethylene hydrogenation reaction by Zaera and Somorjai[5] and in a more generalized scheme by Thomson and Webb.[6] This

(1) Horiuti, J.; Miyahara, K. "Hydrogenation of Ethylene on Metallic Catalysts"; Government Printing Office: Washington, D.C., 1968; NBS-NSRDS No. 13.
(2) Little, L. H. "Infrared Spectra of Adsorbed Species"; Academic: London, 1966; Chapter 5.
(3) Horiuti, J.; Polanyi, M. *Trans. Faraday Soc.* **1934**, *30*, 1164.
(4) Farkas, A.; Farkas, L. *J. Am. Chem. Soc.* **1938**, *60*, 22.
(5) Zaera, F.; Somorjai, G. A. *J. Am. Chem. Soc.* **1984**, *106*, 2288.

0002-7863/86/1508-0663$01.50/0 

proposal has stemmed largely from the recent series of investigations on platinum group single crystals involving the characterization of the ethylidyne species, $\geqslant CCH_3$. This species had never been postulated previously in any mechanism for this reaction; its presence is now well established on both single crystals[7-10] and supported metals[11,12] as a stable surface species formed upon addition of $C_2H_4$ to these metals at room temperature.

The novel mechanism proposed by Zaera and Somorjai[5] involves the surface species ethylidene, $>CHCH_3$, as a hydrogen transfer agent, or "co-catalyst". In their model (see eq 1), the Pt(111) surface is covered with ethylidyne, $\geqslant CCH_3$, which, in the presence

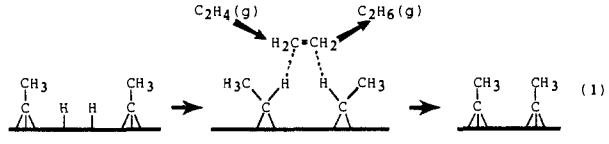


of adsorbed hydrogen, converts to ethylidene, $>CHCH_3$. This ethylidene species then transfers its newly acquired $\alpha$-hydrogen to an ethylene molecule which is adsorbed weakly in the second layer. This process must occur twice per ethylene molecule to completely hydrogenate the ethylene molecule, producing ethane product.

Although there is no direct evidence for the existence of the ethylidene species on these metal surfaces, the authors[5] cite as evidence in support of their model the fact that hydrogenation of ethylene occurs easily on the Pt(111) surface which is covered with ethylidyne species in a (2 × 2) overlayer in UHV prior to and following the hydrogenation of ethylene. In addition, they are able to show that it is the same ethylidyne species which remain on the surface before the reaction as after the reaction by using $^{14}C$-radiotracer methods.[5,13] They find the same steady-state reaction rates for the ethylidyne-precovered surface as when they begin the ethylene hydrogenation reaction on a clean Pt(111) surface and argue that there is a very rapid formation of ethylidyne by the first ethylene molecules to arrive at the surface.

This model is further supported by a more general argument presented earlier by Thomson and Webb[6] in which it was observed that many different metal surfaces give nearly equal rates of ethylene hydrogenation when normalized to the surface area of the exposed metal. They reason that a species, $M-C_xH_y$, acts as a hydrogen transfer agent in $C_2H_4$ hydrogenation. If such a monolayer of adsorbed hydrocarbon species is present on the surface during $C_2H_4$ hydrogenation, and is involved as a hydrogen-transfer co-catalyst, it could be argued that the underlying metal surface would become "masked", and its structure would be of only secondary importance (structure insensitive reaction).

It is an unfortunate consequence of the types of experiments carried out by Zaera and Somorjai[5,13] that their surfaces cannot be examined in any way *during* the high-pressure ethylene hydrogenation experiments. Measurements have been made before and after reaction by moving the sample out of the high-pressure region into UHV for analysis.

In our laboratory, a thorough spectroscopic characterization of the observed ethylidyne and ethylene IR modes on $Pd/Al_2O_3$ has recently been carried out,[11] using procedures which permit direct surface measurements under reaction conditions. In the present paper, we have been able to observe changes occurring on a $Pd/Al_2O_3$ surface *during* the ethylene hydrogenation reaction using transmission infrared spectroscopy. In particular, we have monitored the surface concentration of the ethylidyne species *during* the ethylene hydrogenation reaction starting from various initial surface conditions. We have used the inherently high resolution of the transmission infrared technique in studies of $^{13}C$-ethylidyne and $^{12}C$-ethylidyne species which have characteristic $CH_3$ deformation vibrational frequencies differing by 11 $cm^{-1}$. By simultaneously monitoring ethylene hydrogenation rates and spectroscopically monitoring changes in the surface concentrations of ethylidyne, we reach new conclusions concerning the role of the ethylidyne species in the catalyzed ethylene hydrogenation reaction on Pd catalytic surfaces.

## II. Experimental Section

**A. Preparation of 10% $Pd/Al_2O_3$ Samples.** The sample preparation procedure has been described in detail elsewhere.[14] It consists of impregnation of alumina (Degussa-Aluminum Oxide C, 100 $m^2/g$) with an aqueous–acetone solution of palladium nitrate. The resulting mixture is kept well suspended while it is sprayed from an atomizer onto a 2.54 cm diameter $CaF_2$ sample support plate maintained at ≈340 K. The fine mist hits the $CaF_2$ plate, the solvents flash evaporate, and a uniformly thin layer of metal salt plus alumina is deposited. The mass of Pd employed in these experiments ranges from 0.0022 to 0.0028 g in separate samples.

The $CaF_2$ plate is then transferred to a stainless steel IR cell, where the deposit is first evacuated and heated to 450 K for ~12 h to decompose the nitrate species. Following this, the surface is subjected to four cycles of reduction in hydrogen, each consisting of the following: exposure to 400 torr of $H_2$ at 450 K for 1 h followed by evacuation for 15 min. Following this, a final overnight outgassing is conducted by increasing the cell temperature to ~475 K. Upon cooling, the $Pd/Al_2O_3$ surface is active and ready for experiments. This preparation procedure results in a thin, uncompacted layer which is superior to procedures which involve the use of pressed disks of supported catalysts; effects due to diffusion inside the sample volume are thereby minimized.

CO adsorption experiments at 300 K on these $Pd/Al_2O_3$ surfaces indicate that the monolayer capacity of the Pd is ≅0.12 mol of CO/mol of Pd. Assuming that a distribution of low index Pd planes is exposed in which 0.75 $CO/Pd_s$ will be the average maximum coverage over these planes,[15] the surface area of Pd in our $Pd/Al_2O_3$ preparation is ≅2140 $cm^2$ for a surface containing $3 \times 10^{-3}$ g of Pd. In this paper, we calculate a *total rate* (molecules·$s^{-1}$) of reaction for the $3 \times 10^{-3}$ g Pd surfaces. We also calculate a *specific rate* or areal rate (molecules·$cm^{-2}$·$s^{-1}$), which is shown in parentheses for comparison with specific reaction rates obtained on other surfaces. See ref 18 for more details regarding the Pd substrate.

**B. Apparatus and Spectroscopic Measurements.** An all-stainless-steel gas handling system and infrared cell with a base pressure of $\leqslant 1 \times 10^{-8}$ torr was employed. A liquid nitrogen-cooled sorption pump and a 20 L/s ion pump are used to pump a total system volume of ~600 $cm^3$.

The sample cell for infrared spectroscopic measurements has previously been described.[16] It contains $CaF_2$ optical windows sealed in stainless steel flanges, permitting infrared measurements in the 4000–1000 $cm^{-1}$ spectral range. In addition, the sample temperature can be controlled to within ±2 K over the temperature range of 80 to 600 K.

Infrared spectra were obtained with a purged Perkin-Elmer Model PE-783 infrared spectrophotometer coupled to a 3600 data acquisition system for data storage and manipulation. Spectra presented were obtained with a slit program yielding a maximum resolution of 2.4 $cm^{-1}$ with typical data acquisition times of 80 s/$cm^{-1}$, acquired at 2 points per $cm^{-1}$. In addition, spectra in Figures 5 and 6 were treated with a 19-point smoothing function. The quantitative information extracted from these spectra has not been altered in any way in comparison with the original spectra as a result of the smoothing procedure. Spectroscopic measurements vs. time (Figure 2; Figure 4) were made by setting the spectrometer grating at 1333 or 1322 $cm^{-1}$ and monitoring the signal vs. time. In addition, full scans (4000–1000 $cm^{-1}$) were periodically acquired to rule out gross changes in the spectrum.

Mass spectrometric measurements of the gas phase in the IR cell were made with a Model SM 1000 D Spectrum Scientific, Ltd. quadrupole mass spectrometer with amu peak resolution to the base line over the range of $m/e$ 22 to 32 amu. In each spectrum, a residual gas-phase spectrum recorded immediately prior to the main spectrum has been subtracted. Spectra were recorded by allowing the gas to effuse through

(6) Thomson, S. J.; Webb, G. *J. Chem. Soc., Chem. Commun.* **1976**, 526.
(7) Pt(111): Ibach, H.; Mills, D. L. "Electron Energy Loss Spectroscopy and Surface Vibrations"; Academic: New York, 1982; pp 326–335.
(8) Rh(111): Dubois, L. H.; Castner, D. G.; Somorjai, G. A. *J. Chem. Phys.* **1980**, *72*, 5234.
(9) Pd(111): Kesmodel, L. L.; Gates, J. A. *Surf. Sci.* **1981**, *111*, L747.
(10) Ru(001): Barteau, M. A.; Broughton, J. Q.; Menzel, D. *Appl. Surf. Sci.* **1984**, *19*, 92.
(11) $Pd/Al_2O_3$: Beebe, T. P., Jr.; Albert, M. R.; Yates, J. T., Jr. *J. Catal.* **1985**, *96*, 1.
(12) Sheppard, N.; James, D. I.; Lesiunas, A.; Prentice, J. D. *Commun. Dep. Chem. (Bulg. Acad. Sci.)* **1984**, *17*, 95.
(13) Davis, S. M.; Zaera, F.; Gordon, B. E.; Somorjai, G. A. *J. Catal.* **1985**, *92*, 240.
(14) Yates, J. T., Jr.; Duncan, T. M.; Vaughan, R. W. *J. Chem. Phys.* **1979**, *71*, 3908.
(15) Palazov, A.; Chang, C. C.; Kokes, R. J. *J. Catal.* **1975**, *36*, 338.
(16) Beebe, T. P., Jr.; Gelin, P.; Yates, J. T., Jr. *Surf. Sci.* **1984**, *148*, 526.

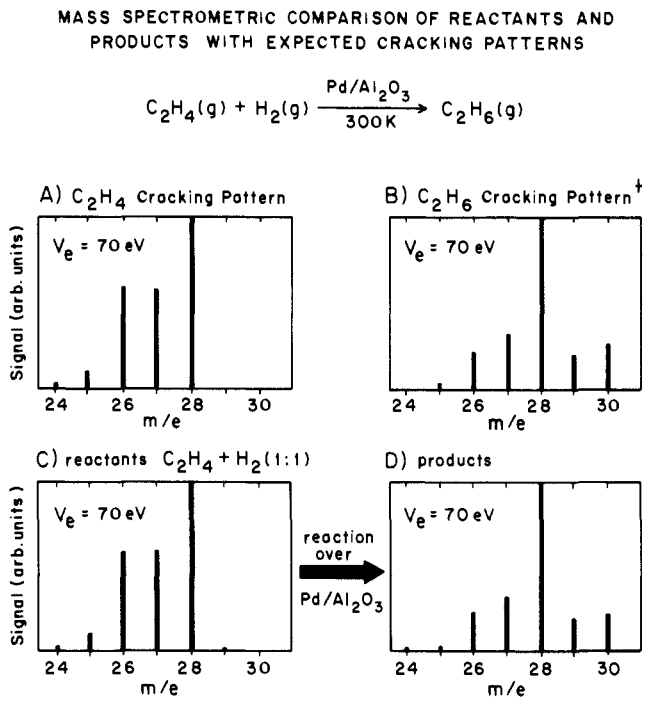


† Atlas of Spectral Data, ed. E. Stenhagen, S. Abrahamsson, and F.W. McLafferty, vol. I, (Wiley, New York) 1969, pg. 5.

**Figure 1.** Mass spectrometric comparison of expected cracking patterns of $C_2H_4(g)$ (A) and $C_2H_6(g)$ (B) with actual spectra of reactants (C) and products (D) of $C_2H_4(g) + H_2(g)$ reaction over $Pd/Al_2O_3$ at 300 K.

a Granville-Phillips leak valve (Model 203) to a steady-state gas pressure of $\sim 1 \times 10^{-7}$ torr in the continuously-pumped region of the quadrupole mass spectrometer.

**C. Gas Handling.** $H_2$ was obtained from Matheson in a high-pressure cylinder at a purity of 99.9995%. Ethylene ($^{12}C_2H_4$) was also obtained from Matheson in a cylinder and transferred to a glass storage bulb at a purity at 99.99%. Ethylene ($^{13}C_2H_4$) was purchased from the MSD Co. with a specified carbon-13 atom content of 92.1% in a break-seal glass bulb.

## III. Results

**A. Mass Spectrometric Analysis of Reactants and Products of the Reaction of $C_2H_4 + H_2$ over $Pd/Al_2O_3$.** Figure 1C shows the 24–30 amu region mass spectrum of an equimolar mixture of $C_2H_4 + H_2$, the reactants prior to exposure to $Pd/Al_2O_3$. As in all presentations in Figure 1, the largest peak has been normalized to 100% of full scale. This reactant mixture is then allowed to contact (static exposure) the $Pd/Al_2O_3$ sample at 300 K for $\geq$10 min. The resulting gas phase is likewise analyzed mass spectrometrically to give the spectrum shown in Figure 1D. Comparison with the standard spectra for $C_2H_4$ and $C_2H_6$ in Figure 1, A and B, shows that quantitative catalytic conversion of $C_2H_4$ to $C_2H_6$ is obtained.

**B. Infrared Spectroscopic Measurements of Ethylidyne and Ethylene Hydrogenation.** The hydrogenation of ethylene has been studied both on surfaces initially containing no ethylidyne (Figure 2) and on surfaces initially containing a maximum coverage of ethylidyne (Figure 4). In Figure 2 and its associated table, it can be seen that for reaction of $C_2H_4 + H_2$ over $Pd/Al_2O_3$, the relative initial amount of $C_2H_4$ and $H_2$ is crucial in determining whether or not ethylidyne forms on the surface during the ethylene hydrogenation reaction. It can be seen that for $P^\circ_{C_2H_4}/P^\circ_{H_2} \lesssim 1.5$ (experiments 1–8), no detectable level of ethylidyne has formed, whereas when there is an excess of ethylene relative to hydrogen (experiments 9–12), the rate of ethylidyne formation on the Pd surface is strongly dependent on the amount of excess ethylene.

The maximum slope listed in column 2 of Figure 2 can be related to a maximum rate of formation of ethylidyne when $\epsilon_{1333\ cm^{-1}}$ (absorbance·molecule$^{-1}$) is known for the ethylidyne surface species. In separate experiments, we have attempted to measure

**Table I.** Ethylene Hydrogenation on $Pd/Al_2O_3$: Measurement of Kinetic Orders with Respect to $C_2H_4$ and $H_2$

$$C_2H_4(g) + H_2(g) \xrightarrow{Pd/Al_2O_3} C_2H_6(g)$$

$$\text{rate} = k(P^\circ_{H_2})^a(P^\circ_{C_2H_4})^b$$

| $T$, K | $a$ | $b$ | $P^\circ_{H_2}$, torr | $P^\circ_{C_2H_4}$, torr |
|---|---|---|---|---|
| 298 | 0.84 ± 0.1 | | 0.050 → 0.200 | 0.050 |
| 298 | 0.98 ± 0.05 | | 0.050 → 0.200 | 0.050 |
| 298 | 0.95 ± 0.05 | | 0.100 → 0.400 | 0.100 |
| 298 | 0.93 ± 0.1 | | 0.100 → 0.400 | 0.100 |
| 298 | | −0.3 ± 0.1 | 0.100 | 0.150 → 0.400 |
| 292 | | 0.05 ± 0.1 | 0.150 | 0.040 → 0.180 |
| 292 | | 0.00 ± 0.1 | 0.150 | 0.040 → 0.180 |

**Table II.** Measurement of Initial Rates[a] of Hydrogenation on $Pd/Al_2O_3$ Surfaces with and without Ethylidyne

| | initial pressures[b] | | with *preadsorbed* ethylidyne | | without ethylidyne | |
|---|---|---|---|---|---|---|
| $T$, K | $H_2$ | $C_2H_4$ | specific rate[c] | turnover no.[d] | specific rate[c] | turnover no.[d] |
| 279 | 0.997 | 0.997 | 2.15 | 0.017 | 2.15 | 0.017 |
| 292 | 0.150 | 0.040 | 5.18 | 0.041 | 5.34 | 0.042 |
| 292 | 0.150 | 0.070 | 5.18 | 0.041 | 5.65 | 0.045 |
| 292 | 0.150 | 0.100 | 5.39 | 0.043 | 4.82 | 0.038 |
| 292 | 0.150 | 0.130 | 5.85 | 0.046 | 5.39 | 0.043 |
| 292 | 0.150 | 0.150 | 5.75 | 0.045 | 5.18 | 0.041 |
| 292 | 0.150 | 0.180 | 5.44 | 0.043 | 5.60 | 0.044 |

[a] Estimated errors in rates are ±6%. [b] Initial pressures in torr. [c] Specific rates in molecules·cm$^{-2}$·s$^{-1}$ × $10^{-13}$. [d] Turnover number in molecules·s$^{-1}$·Pd$_s^{-1}$, using assumptions in ref 18.

$\epsilon_{1333\ cm^{-1}}$ for ethylidyne by correlating the $C_2H_4$ adsorption isotherm to the measured ethylidyne IR absorbance. By assuming in $C_2H_4$ adsorption experiments that in the first small exposures of ethylene to the clean $Pd/Al_2O_3$ surface all ethylene which chemisorbs is converted to ethylidyne, this initial slope may be used to determine $\epsilon_{1333\ cm^{-1}}$, the absorbance per ethylidyne molecule. The value deduced in this manner is $\epsilon_{1333\ cm^{-1}} = 7 \times 10^{-20}$ absorbance·molecule$^{-1}$.

As an example, the maximum rate of ethylidyne production in experiment 9 in Figure 2 can be calculated as follows:

$$\text{slope}_{max} \times \frac{1}{\epsilon_{1333\ cm^{-1}}} = \text{rate}$$

$$1.2 \times 10^{-5}\ \frac{\text{Abs}}{\text{s}} \times \frac{\text{molecule}}{(7 \times 10^{-20})\text{Abs}} = 1.7 \times 10^{14}\ \frac{\text{molecule}}{\text{s}}\ (\pm 20\%) \quad (2)$$

(This corresponds to a specific rate of formation of ethylidyne $\cong 1 \times 10^{11}$ molecules·cm$^{-2}$·s$^{-1}$.)

Figure 3A shows how the inherently high resolution transmission IR experiment can be exploited to study mixtures of $^{12}C$-ethylidyne and $^{13}C$-ethylidyne on our $Pd/Al_2O_3$ surfaces. These two isotopic surface species have symmetric methyl deformation modes which are $\sim$11 cm$^{-1}$ apart and easily resolved at the 2.4-cm$^{-1}$ resolution employed here. Spectrum a in Figure 3A was obtained by adsorption of $\sim 1.4 \times 10^{17}$ molecules of $^{13}C_2H_4$ on a clean $Pd/Al_2O_3$ surface at 293 K. Likewise, spectrum b in Figure 3A was obtained from a clean $Pd/Al_2O_3$ surface onto which $\sim 2.6 \times 10^{17}$ $^{12}C_2H_4$ molecules were adsorbed. Spectrum c in Figure 3A was obtained following the adsorption of $\sim 8 \times 10^{17}$ molecules from a 1:1 mixture of $^{13}C_2H_4$ and $^{12}C_2H_4$, followed by evacuation.

Figure 3B shows the schematic design of the next series of experimental results to be described. The $^{13}C$-surface ethylidyne species is formed to its maximum level by exposure of the surface to $^{13}C_2H_4$ at 300 K. Ethylene hydrogenation is then conducted above this surface by addition of $^{12}C_2H_4$ and $H_2$ (1:1),yielding various products, as shown in Figure 3B.

Seven such experiments above a $^{13}C$-ethylidyne layer were performed, each starting with different amounts of $^{12}C_2H_4 + H_2$

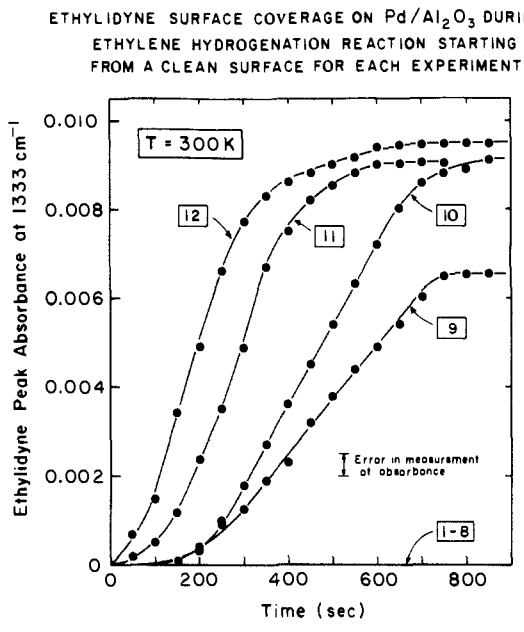


| Experiment No. | Maximum Slope (Abs·sec$^{-1}$·$10^5$) | $P^0(C_2H_4)$ (Torr) | $\frac{P^0(C_2H_4)}{P^0(H_2)}$ | Maximum Rate of Ethylidyne Production (molec·sec$^{-1}$·$10^{-14}$) |
|---|---|---|---|---|
| 1-7 | 0 | 0.025-0.100 | 0.25-1.00 | 0 (±10%) |
| 8 | 0 | 0.150 | 1.50 | 0 |
| 9 | 1.2 | 0.200 | 2.00 | 1.7 |
| 10 | 1.8 | 0.250 | 2.50 | 2.6 |
| 11 | 2.9 | 0.300 | 3.00 | 4.1 |
| 12 | 3.4 | 0.350 | 3.50 | 4.9 |

$P^0(H_2)$ = 0.100 Torr

**Figure 2.** Development of surface ethylidyne species during ethylene hydrogenation reactions begun on clean $Pd/Al_2O_3$ surfaces. Experiments 1–12 were each begun with different amounts of ethylene relative to hydrogen, as shown in the accompanying table.

(1:1). These amounts of gas correspond to initial pressures ranging from 0.017 to 3.418 torr. Hydrogenation rates were not measured for these particular experiments, but typical rates of analogous experiments are given in Table II. The results in Figure 4 and its associated table reveal that the removal of $^{13}C$-ethylidyne with time is closely related to the initial quantity of $^{12}C_2H_4 + H_2$ (1:1) which is exposed to the Pd surface. For experiments 1 and 2, where $\sim 2 \times 10^{17}$ $^{12}C_2H_4$ molecules are employed, there is no change in the $^{13}C$-ethylidyne surface concentration with time, whereas for experiment 7, where $3.3 \times 10^{19}$ $^{12}C_2H_4$ molecules are employed, the rate of removal of $^{13}C$-ethylidyne species is nearly $2 \times 10^{15}$ molecules·s$^{-1}$ initially ($1.1 \times 10^{12}$ molecules·cm$^{-2}$·s$^{-1}$).

In these same experiments, we have recorded a high-resolution IR spectrum before and after each exposure of $^{12}C_2H_4 + H_2$ (1:1) to the surface initially containing a maximum coverage of $^{13}C$-ethylidyne. These data are shown in Figure 5. By subtracting the spectrum before the hydrogenation reaction from the spectrum after the hydrogenation reaction, a series of difference spectra are obtained (Figure 6) which clearly reflect the changes which occur on Pd as a result of the reaction. We have plotted these difference spectrum peak areas as a function of the number of $^{12}C_2H_4$ molecules initially admitted to the $Pd/Al_2O_3$ sample in Figure 7. Here it is seen that the surface concentration of $^{13}C$-ethylidyne monotonically decreases as greater amounts of $^{12}C_2H_4$ are hydrogenated. The surface concentration of $^{12}C$-ethylidyne produced by reaction can be seen to go through a maximum value following the hydrogenation of $\sim 6 \times 10^{18}$ $^{12}C$-ethylene molecules. For amounts larger than this, little or no $^{12}C$-ethylidyne remains on the surface following hydrogenation.

**C. Rate Measurements of Ethylene Hydrogenation on Surfaces with and without Ethylidyne.** We have measurements of the kinetic orders with respect to $C_2H_4$ and $H_2$ above our $Pd/Al_2O_3$ surface. The details of the procedure used are described in the Appendix.

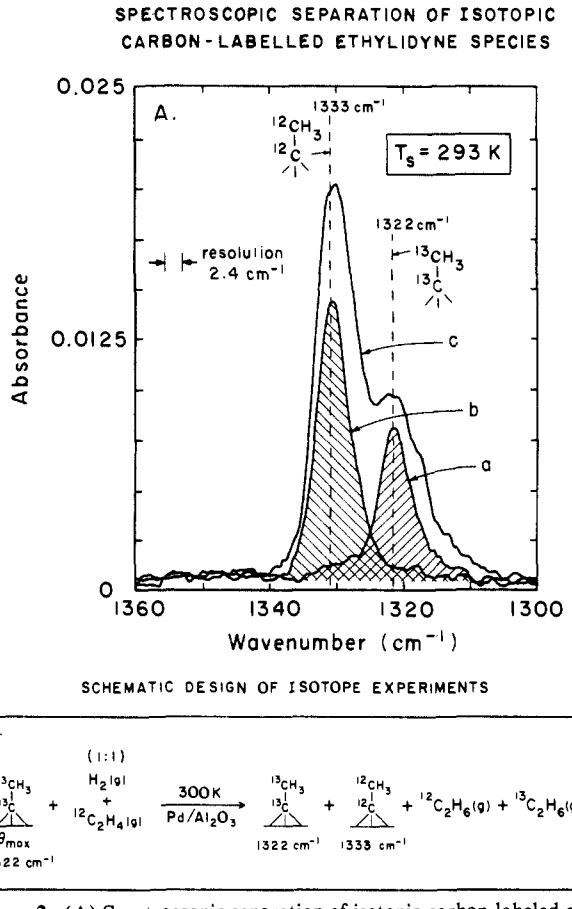


**Figure 3.** (A) Spectroscopic separation of isotopic carbon-labeled ethylidyne species on $Pd/Al_2O_3$. Spectrum a obtained following adsorption of $1.35 \times 10^{17}$ $^{13}C_2H_4$ molecules on clean $Pd/Al_2O_3$ surface. Likewise, spectrum b obtained following adsorption of $2.59 \times 10^{17}$ $^{12}C_2H_4$ molecules on clean surface. Spectrum c obtained after adsorption of $\approx 8.1 \times 10^{17}$ molecules from a 1:1 mixture of ($^{13}C$) and ($^{12}C$)ethylene, followed by evacuation. (B) Schematic design of isotope experiments to study ethylidyne surface species during ethylene hydrogenation.

The results, tabulated in Table I, show an approximately first-order dependence on hydrogen pressure and an approximately 0-order dependence on ethylene pressure.

We have previously shown in Figure 2 that it is possible to conduct ethylene hydrogenation experiments above a $Pd/Al_2O_3$ surface without ever forming a measurable concentration of surface ethylidyne. The conditions required are only that the relative amount of ethylene to hydrogen is less than or equal to $\sim 1.5$; i.e., $N^\circ_{C_2H_4}/N^\circ_{H_2} \lesssim 1.5$.

Using this convenient feature we have been able to accurately measure ethylene hydrogenation rates above $Pd/Al_2O_3$ surfaces *without* and *with* saturation coverages of ethylidyne, but identical in all other respects. These data are shown in Table II where it can be seen that the measured initial rates of hydrogenation are the same, within experimental error, for surfaces with and without preadsorbed ethylidyne.

Reaction rates for the ethylene hydrogenation reaction have likewise been measured with $H_2$ vs. $D_2$ as a reactant gas, over a broad temperature range as shown in Figure 8. The reaction exhibits rates which are $\sim 1.3$ times faster for $H_2$ than for $D_2$ and shows a *decrease* in rate with increasing temperature. These features will be discussed below.

## IV. Discussion

**A. Mass Spectrometric Analysis of Reactants and Products.** In Figure 1, A and B, we present the cracking patterns expected for pure $C_2H_4$ and $C_2H_6$, respectively, for comparison with the C and D spectra of Figure 1. The agreement between spectra A and C and between B and D in Figure 1 demonstrates the complete catalytic conversion of $C_2H_4$ over the $Pd/Al_2O_3$ surface for 1:1 mixtures of $H_2$ and $C_2H_4$. During a given reaction, the

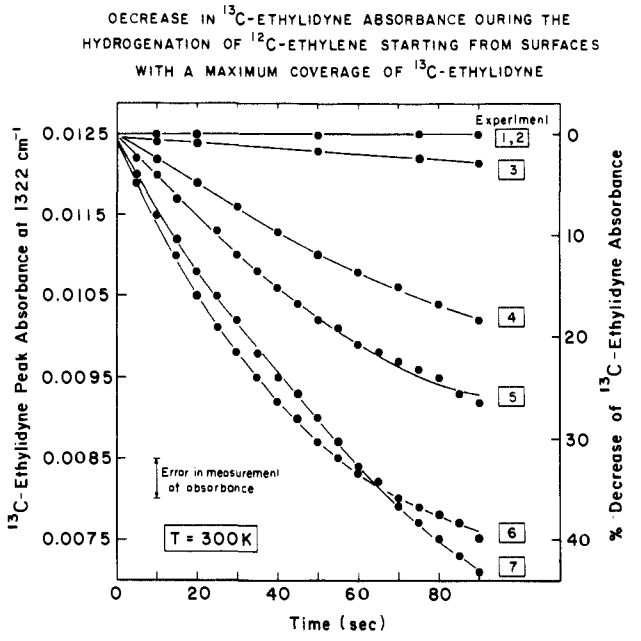


| Experiment No. | Initial Number of Gas Phase $^{12}C_2H_4$ and $H_2$ molecules ($\times 10^{-17}$) | Initial Rate of Removal of $^{13}C$-Ethylidyne (molec·sec$^{-1}$·$10^{-14}$) |
|---|---|---|
| 1 | 1.7 | 0 (±3) |
| 2 | 3.3 | 0 |
| 3 | 13.2 | 1 |
| 4 | 33.0 | 6 |
| 5 | 97.2 | 10 |
| 6 | 160.0 | 20 |
| 7 | 330.0 | 17 |

**Figure 4.** Decrease in surface concentration of ($^{13}C$)ethylidyne species measured *during* ($^{12}C$)ethylene hydrogenation reactions begun on surfaces containing a maximum coverage of ($^{13}C$)ethylidyne. Experiments 1–7 were begun with 1:1 mixtures of increasingly greater amounts of $C_2H_4$(g) and $H_2$(g), as shown in the accompanying table.

pressure asymptotically approaches one-fourth of its initial value. One-half of this effect is due to the doubling of the system volume (see Appendix, Figure 9). The remaining half of the pressure drop can be attributed to the gas-phase stoichiometry of the ethylene hydrogenation reaction: 2 moles(g) → 1 mole(g). These data and the mass spectrometric data confirm that we are observing the hydrogenation of ethylene and that there is a quantitative conversion of ethylene to ethane.

**B. In Situ Infrared Spectroscopic Measurements of Ethylidyne Surface Concentration during Ethylene Hydrogenation. 1. Surfaces Initially Free of Ethylidyne.** Figure 2 and its associated table show the data from ethylene hydrogenation reactions begun on surfaces which were initially clean. In experiments 1–8 there was no detectable development of surface ethylidyne during ethylene hydrogenation. In experiments 9–12, where there is an excess of $C_2H_4$ relative to $H_2$, the increase of ethylidyne surface concentration with time is an increasing function of the amount of excess $C_2H_4$. Experiments 1–8 demonstrate for the first time that ethylene conversion to ethylidyne is kinetically much less favorable than ethylene hydrogenation in the presence of hydrogen at 300 K on $Pd/Al_2O_3$. Indeed, this is borne out in experiments 9–12 (see table in Figure 2) where the maximum rates of formation of ethylidyne during ethylene hydrogenation approach only $5 \times 10^{14}$ ethylidyne·s$^{-1}$ ($2.8 \times 10^{11}$ molecules·cm$^{-2}$·s$^{-1}$). This rate is two to three orders of magnitude slower than the ethylene hydrogenation rate in these reactions which is typically $10^{16}$ to $10^{17}$ molecules·s$^{-1}$ ($6 \times 10^{12}$–$6 \times 10^{13}$ molecules·cm$^{-2}$·s$^{-1}$), to be discussed below. We can conclude from these results that the ethylidyne species is not a direct intermediate in the hydrogenation of ethylene on $Pd/Al_2O_3$ since its rate of formation is orders of magnitude slower than the production rate of ethane.

In a related argument by Zaera and Somorjai[5] and Berlowitz et al.,[17] the measured rate of hydrogenation of ethylidyne on Pt(111) was much slower than the hydrogenation of ethylene, also confirming that ethylidyne is not a direct intermediate in the

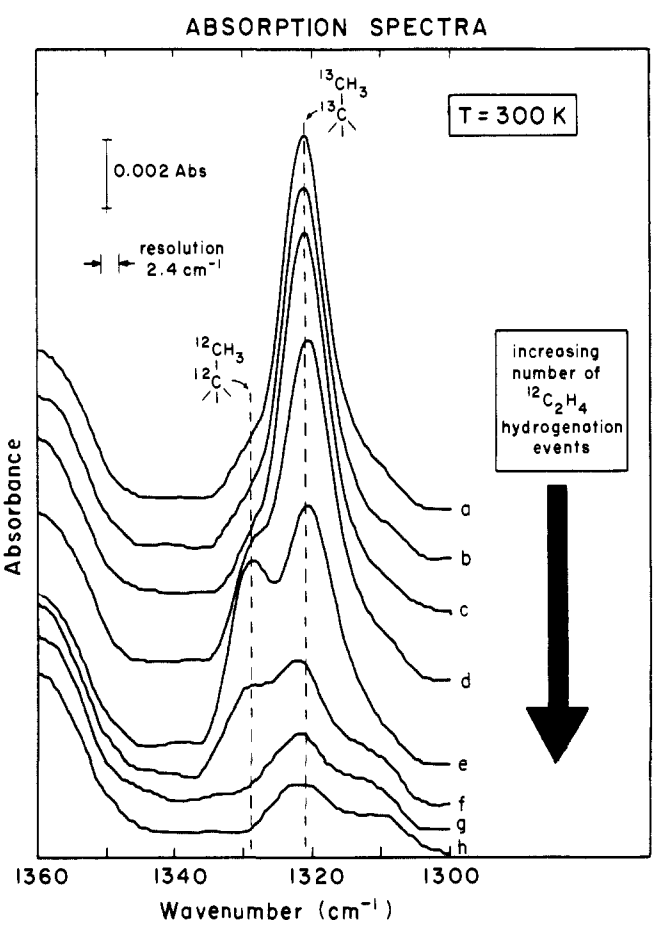


**Figure 5.** IR spectra obtained *following* the hydrogenation of increasingly greater amounts of $^{12}C_2H_4 + H_2$ (1:1) begun on surfaces initially containing a maximum coverage of $^{13}C$-ethylidyne. Spectrum a obtained from this surface prior to any reaction, while spectra b–h correspond respectively to experiments 1–7 of Figure 4 and its accompanying table.

hydrogenation mechanism on Pt(111) surfaces. In addition, when the deuterium content of the ethane resulting from reaction of $C_2H_4 + D_2$ is followed on Pt(111), the maximum average deuterium incorporation is between 1 and 2 deuterium atoms per ethane.[5] This result supports an associative adsorption mechanism for the ethylene and precludes the involvement of ethylidyne as a direct intermediate, since the resulting ethane in the latter case would be expected to contain, on average, three deuterium atoms. These considerations are illustrated below.

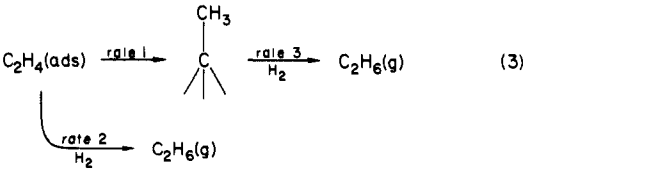


| $Pd/Al_2O_3$ (results from this work) | Pt(111) (results from Zaera and Somorjai[5]) |
|---|---|
| rate 2 >> rate 1 (Figure 2) | |
| rate 2 >> rate 3 (to be discussed, Figure 4) | rate 2 >> rate 3 |

**2. Surfaces Initially Containing a Maximum Coverage of Ethylidyne.** In this series of experiments we have made use of two advantages of optical spectroscopic techniques (high resolution; in situ probe), for studies of $^{13}C$-ethylidyne and $^{12}C$-ethylidyne on $Pd/Al_2O_3$ surfaces during reaction at relatively high pressures.

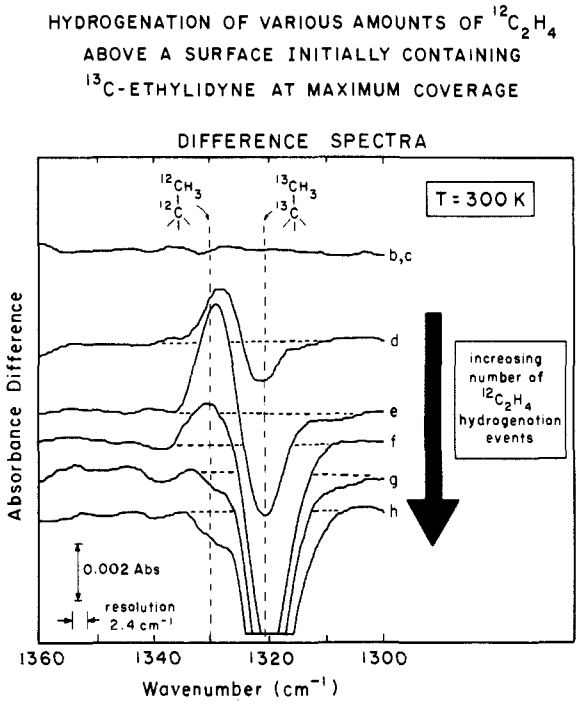


Figure 6. IR difference spectra obtained from subtraction of spectrum a in Figure 5 from each of spectra b–h in Figure 5. That is, Figure 6d = Figure 5d - Figure 5a, etc. See also the captions for Figures 4 and 5.

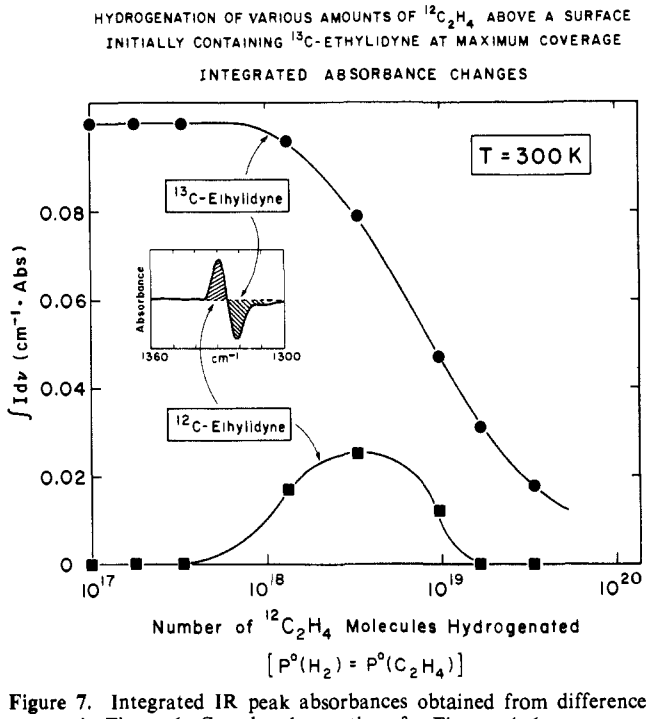


Figure 7. Integrated IR peak absorbances obtained from difference spectra in Figure 6. See also the captions for Figures 4–6.

The schematic design of these experiments is illustrated in Figure 3, A and B.

In distinction from the experiments of Figure 2 which were begun on surfaces free of ethylidyne, this series of experiments was begun on $Pd/Al_2O_3$ surfaces which contain a maximum coverage of ethylidyne. It is incorrect to think of such a surface as the supported surface analogue of a saturated (111) single-crystal surface which is covered with a (2 × 2) overlayer of ethylidyne as determined by LEED.[5] This is because $Pd/Al_2O_3$ preparations will certainly contain a variety of exposed crystal planes, including Pd(111). Our $Pd/Al_2O_3$ crystallites have an average particle size of 75 Å based on CO adsorption isotherm measurements.[18] Competition experiments between ≻C–$CH_3$ and CO suggest that about 15% of the surface of these Pd crystallites

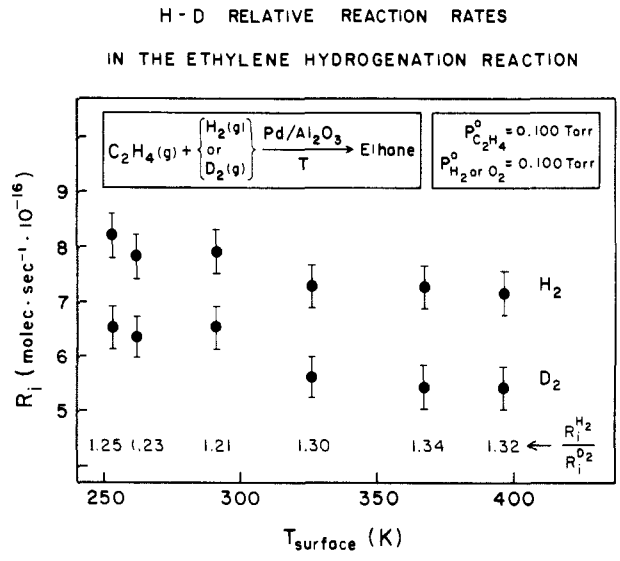


Figure 8. Observation of a H–D kinetic isotope effect in the ethylene hydrogenation reaction on $Pd/Al_2O_3$ for various temperatures.

is covered with ethylidyne at saturation.[18] The remaining 85% of the surface which is not—and cannot be—covered with ethylidyne is available for chemisorption of ethylene and hydrogen.

With this in mind, the experiments in Figure 4 have each been started on a surface containing ≈5 × $10^{17}$ $^{13}C$-ethylidyne moelcules (~2.8 × $10^{14}$ moelcules·$cm^{-2}$), the maximum coverage which can be obtained for these surfaces. In situ monitoring of the $^{13}C$-ethylidyne peak absorbance vs. time during the hydrogenation of various quantities of $^{12}C_2H_4 + H_2$ (1:1) reveals that the removal rate of $^{13}C$-ethylidyne is roughly proportional to the number of reactant $^{12}C_2H_4 + H_2$ molecules (see table in Figure 4). On the basis of arguments presented in the following paragraph, we believe that the partial pressure of $H_2$ (and not $C_2H_4$) is the crucial factor in determining the rate of ethylidyne removal. During the hydrogenation of small quantities of ethylene (experiments 1 and 2, Figure 4), there is no detectable change in the surface concentration of $^{13}C$-ethylidyne species. As greater quantities of $^{12}C_2H_4 + H_2$ (1:1) are hydrogenated, $^{13}C$-ethylidyne is removed at higher rates, due to the increased pressure of $H_2$. Maximum rates of ethylidyne removal of ~20 × $10^{14}$ molecules·$s^{-1}$ (~1.1 × $10^{12}$ molecules·$cm^{-1}$·$s^{-1}$) are slightly faster than the ethylidyne formation rates (Figure 2), which allow the relative rates of eq 3 to be ranked in the order rate 1 ≲ rate 3 << rate 2.

The observed decrease in $^{13}C$-ethylidyne surface concentration during the ethylene hydrogenation reaction could possibly occur by two different elementary steps as shown in eq 4. We have

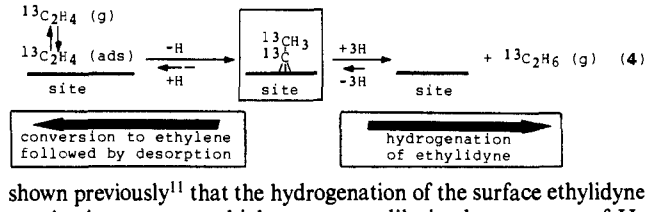


shown previously[11] that the hydrogenation of the surface ethylidyne species is a process which occurs readily in the presence of $H_2$ at 300 K. The process on the left-hand side of eq 4, conversion of ethylidyne to ethylene followed by desorption, does not occur significantly. If the equilibria pictured in the left side of eq 4 did exist, evacuation of a surface partially covered by ≻$CCH_3$, H(ads), and $C_2H_4$(ads) in equilibrium with $C_2H_4$(g) should lead to a decrease in the surface coverage of ≻$CCH_3$. This is not observed. For this reason, we view the removal of surface ethylidyne species in the presence of $C_2H_4 + H_2$ (1:1) as one of ethylidyne hydrogenation, which is occurring in a slow, unrelated process along with the much faster ethylene hydrogenation reaction.

This reaction scheme (eq 4) is supported by the high-resolution (relative to electron energy loss spectroscopy) IR spectra obtained before and after each of the reactions in Figure 4. These spectra

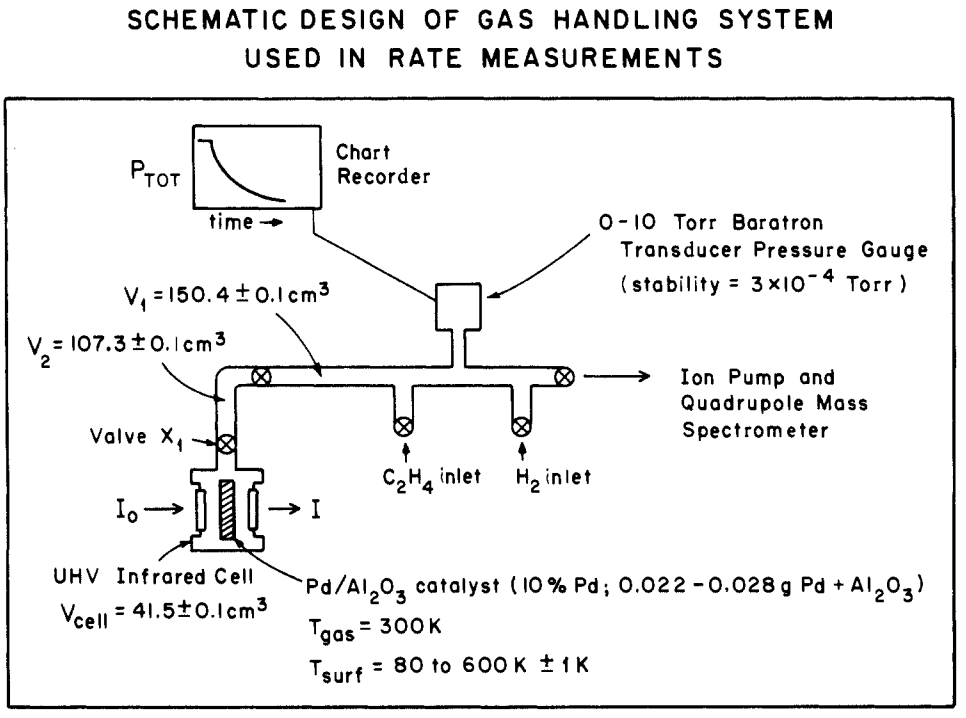


**Figure 9.** Schematic design of the gas handling system used in rate determinations and IR measurements.

are presented in Figures 5 and 6. The absorbance peak areas of the difference spectra in Figure 6 are shown in Figure 7. The hydrogenation of greater amounts of $^{12}C_2H_4 + H_2$ (1:1) means that initially there is a higher pressure $H_2$ which leads to *faster* removal of $^{13}C$-ethylidyne (Figure 4) and to greater amounts of $^{13}C$-ethylidyne removal by the end of the $C_2H_4$ hydrogenation reaction (Figure 7). The plot of the $^{12}C$-ethylidyne peak areas after each of these reactions shows that the surface concentration of these species goes through a maximum at an intermediate value of $^{12}C_2H_4$ molecules hydrogenated. This is also reasonable since when $^{13}C$-ethylidyne species are hydrogenated leaving a vacant site, the vast majority of gas-phase ethylene molecules are $^{12}C_2H_4$. Adsorption of these molecules on this site would lead to the formation of $^{12}C$-ethylidyne. This newly-formed $^{12}C$-ethylidyne species is then itself vulnerable to hydrogenation as more $H_2$ is available in moving to the right in Figure 7. It is reasonable that the steepest slope (Figure 7) in the removal of $^{13}C$-ethylidyne corresponds roughly to the greatest number of $^{12}C$-ethylidyne formed (Figure 7) for the reasons discussed above, including replacement by $^{12}C_2H_4(g)$.

The influence of $D_2$ substitution for $H_2$ on the kinetics of the ethylene hydrogenation on $Pd/Al_2O_3$ is shown in Figure 8. The factor of $R_H/R_D \cong 1.3$, which we measure on the $Pd/Al_2O_3$, has also been reported for this reaction on Pt(111) by Zaera and Somorjai.[5] This deuterium kinetic isotope effect can result from either of two possible mechanisms. (1) In the limit of low equilibrium hydrogen coverages, for nonactivated $H_2$ adsorption,[19] the effect could be ascribed to the arrival rate differences for $H_2$ and $D_2$ which results from the dependence of the average molecular velocities on $M^{1/2}$. (2) In the limit of a saturated hydrogen coverage under reaction conditions, the kinetic isotope effect could be related to zero-point vibrational energy differences for chemisorbed H and D on Pd. In the temperature range of the experiments of Figure 8 (260–390 K), based on TPD measurements for H/Pd(111)[20] and H/Pd ribbon,[21] it is more likely that mechanism (2) may be operative in the 0.1 torr hydrogen pressure range, leading to the deuterium kinetic isotope effect.

The observed decrease in reaction rate with temperature has prevented us from obtaining a meaningful activation energy. It suggests that the equilibrium surface concentration of reactant species such as H(ads) or $C_2H_4$(ads) decreases as temperature increases, leading to the lower rates.

**C. Rate Measurements of the Ethylene Hydrogenation Reaction on Surfaces with and without Ethylidyne.** In Table I our measured kinetic orders with respect to ethylene and hydrogen of ~0 and ~1, respectively, are in close agreement with results obtained by others.

Initial $C_2H_4$ hydrogenation rates reported in Table II for $Pd/Al_2O_3$ surfaces initially contained no ethylidyne and surfaces initially containing a maximum coverage of ethylidyne are the same within experimental error (±6%). Previously reported turnover numbers for ethylene hydrogenation on $Pt/SiO_2$ are 0.05 to 0.22 molecules·$s^{-1}$·$Pt_s^{-1}$ at 223 K[22] and ≅1 molecules·$s^{-1}$·$Pt_s^{-1}$ at 300 K on Pt(111).[5] Typical turnover numbers reported in Table II are on the order of 0.04 molecules·$s^{-1}$·$Pd_s^{-1}$. The fact that the ethylene hydrogenation reaction proceeds in the absence of any ethylidyne (sensitivity level would allow us to detect $\gtrsim 1 \times 10^{16}$ ethylidyne species, whereas these catalyst surfaces typically have $\sim 3 \times 10^{18}$ sites) and that the hydrogenation proceeds with rates which are the same as for any other surface condition suggests that *the ethylidyne species is a spectator surface species in the ethylene hydrogenation reaction on $Al_2O_3$ supported Pd catalytic surfaces such as those employed in this study.* Furthermore, this suggests that the mechanism proposed by Zaera and Somorjai[5] in which the *ethylidene* species, $>CHCH_3$, participates as a "co-catalyst" proceeding from the *ethylidyne* species, eq 1, is not a significantly important pathway for ethylene hydrogenation on typical catalysts such as the $Pd/Al_2O_3$ samples employed here.

(17) Berlowitz, P.; Megiris, C.; Butt, J. B.; Kung, H. H. *Langmuir* **1985**, *1*, 206.

(18) Beebe, T. P., Jr.; Yates, J. T., Jr., work in progress. The monolayer CO capacity of a typical $Pd/Al_2O_3$ sample of mass $2.93 \times 10^{-2}$ g (10% Pd) is $3.32 \times 10^{-6}$ mole CO. Assuming a value of 0.75 C/$Pd_s$ (ref 15), this indicates a dispersion $D$ of

$$D = \frac{\text{mol of CO at saturation}}{(\text{mol of CO/mol of Pd}_s)\text{mol of Pd}_{TOT}} = 0.16$$

The average particle size of the Pd crystallites $\bar{d}$ is given by

$$\bar{d} = \frac{6}{D}\frac{V_{Pd}}{A_{Pd}} \cong 75 \text{ Å}$$

where $V_{Pd}$ is the volume of a Pd atom in the bulk (15.5 Å$^3$) and $A_{Pd}$ is the average area of a Pd atom in the surface, for the main low index planes (7.9 Å$^2$).

(19) Engel, T.; Kuipers, H. *Surf. Sci.* **1979**, *90*, 162.

(20) Conrad, H.; Ertl, G.; Latta, E. *Surf. Sci.* **1974**, *41*, 435.

(21) Kiskinova, M.; Bliznakov, G.; Surnev, L. *Surf. Sci.* **1980**, *94*, 169.

(22) Schlatter, J. C.; Boudart, M. *J. Catal.* **1972**, *24*, 482.

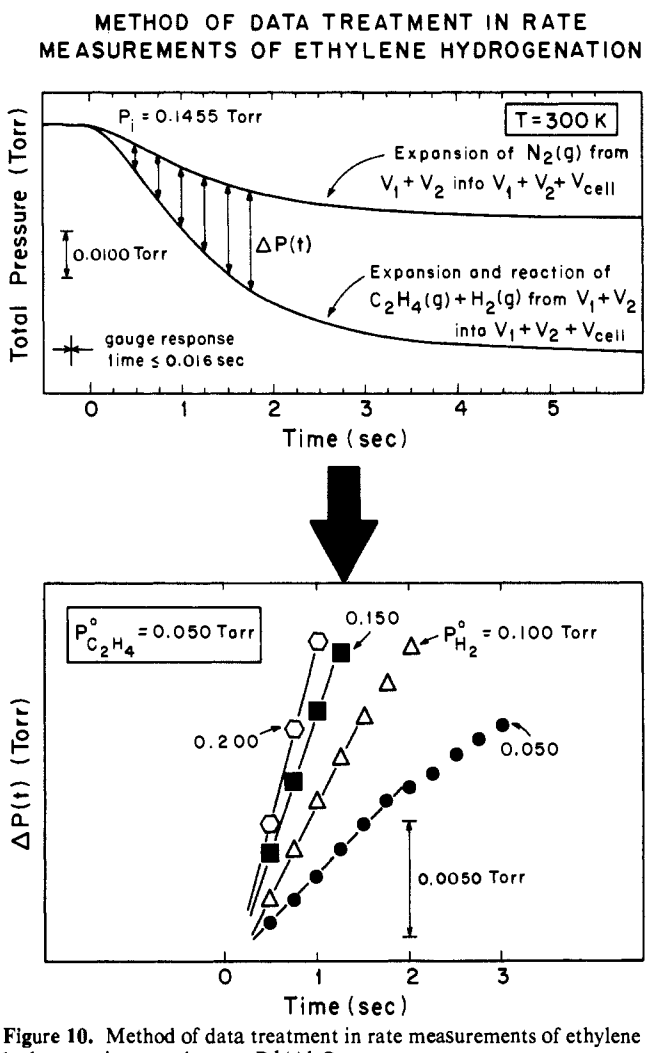


Figure 10. Method of data treatment in rate measurements of ethylene hydrogenation reactions on $Pd/Al_2O_3$.

In this work we have shown that $C_2H_4$ hydrogenation proceeds on a $Pd/Al_2O_3$ catalyst without cognizance of the presence or absence of surface ethylidyne. Since it is likely that only a fraction of the surface sites on the $Pd/Al_2O_3$ catalyst involve ethylidyne, the work does not address the mechanism of $C_2H_4$ hydrogenation on sites which do not form an ethylidyne overlayer.

## V. Summary of Results

The following results have been obtained in the study of $C_2H_4$ hydrogenation on supported $Pd/Al_2O_3$ surfaces.

1. The reaction of $C_2H_4 + H_2$ (1:1) has been shown to proceed quantitatively to completion at 300 K, producing $C_2H_6$ product.

2. For $C_2H_4 + H_2$ gas mixtures with $C_2H_4$ in excess of $H_2$, the kinetics of the buildup of surface ethylidyne (≥C–$CH_3$) can be followed spectroscopically by using the $\delta_s(CH_3)$ vibrational mode at 1333 $cm^{-1}$ characteristic of ethylidyne.

3. Under conditions where equal or excess gas-phase $H_2$ exists compared to $C_2H_4$, surface ethylidyne is not formed during reaction, as indicated by infrared measurements made during reaction.

4. The initial rate of hydrogenation of $C_2H_4$ on $Pd/Al_2O_3$ catalysts is independent of the presence of surface ethylidyne, suggesting that ethylidyne is a spectator species not essential to $C_2H_4$ hydrogenation.

5. Isotopically labeled surface ethylidyne (≥$^{13}C$–$^{13}CH_3$) may be measured by infrared spectroscopy in the presence of unlabeled ethylidyne by using the $\delta_s(CH_3)$ mode at 1322 $cm^{-1}$. Hydrogenation (300 K) of $^{12}C_2H_4$ takes place at a rapid rate compared to replacement of $^{13}C$-labeled ethylidyne by $^{12}C$-ethylidyne.

6. Transmission IR spectroscopy, combined with kinetic methods, is a powerful tool for in situ studies of the involvement of surface species in heterogeneous catalytic reactions. This method offers distinct advantages over those surface science methods which work only in ultrahigh vacuum.

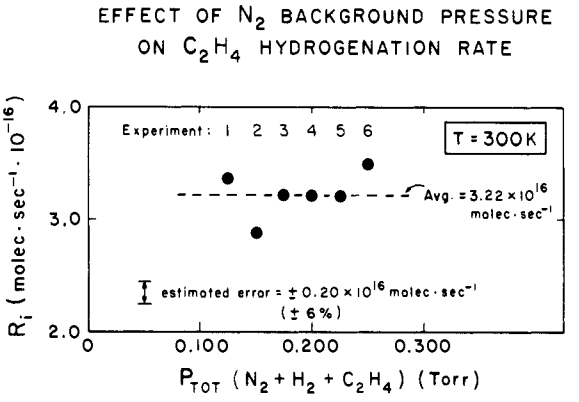


| Experiment | Initial Pressure (Torr) $H_2$ | $C_2H_4$ | $N_2$ | Total | $R_i$ (molec·$sec^{-1}$·$10^{-16}$) |
|---|---|---|---|---|---|
| 1 | 0.0500 | 0.0500 | 0.0250 | 0.1250 | 3.36 ± 0.2 |
| 2 | 0.0500 | 0.0500 | 0.0500 | 0.1500 | 2.87 |
| 3 | 0.0500 | 0.0500 | 0.0750 | 0.1750 | 3.21 |
| 4 | 0.0500 | 0.0500 | 0.1000 | 0.2000 | 3.21 |
| 5 | 0.0500 | 0.0500 | 0.1250 | 0.2250 | 3.21 |
| 6 | 0.0500 | 0.0500 | 0.1500 | 0.2500 | 3.48 |

Figure 11. Confirmation of lack of diffusion-related effect on rate measurements; $N_2$ background pressure increased in experiments 1–6 (see the accompanying table).

**Acknowledgment.** The authors acknowledge with thanks the support of this work by the Science Research Laboratories and the 3M Central Research Laboratories. We also acknowledge helpful discussions with Drs. Mark Albert, John Crowell, Allen Siedle, and Francisco Zaera.

## Appendix: Measurement of Initial Rates for the Ethylene Hydrogenation Reaction

In this appendix we show, in some detail, the methods used in measurements of initial rates for the ethylene hydrogenation reaction:

$$C_2H_4(g) + H_2(g) \xrightarrow{Pd/Al_2O_3\ (10\%)} C_2H_6(g) \qquad (5)$$

By carefully controlling the initial pressures of reactants and monitoring the pressure drop during reaction, rate information can be extracted.

Pressure measurements were made with a 0–10 torr Model 221A Baratron absolute pressure transducer (MKS Instruments) with a time constant ≤$16 \times 10^{-3}$ s and an accuracy of ±0.5% of reading. The transducer is carefully insulated to prevent rapid temperature changes due to air currents surrounding the transducer head. The experimental setup is shown schematically in Figure 9. Initial pressures of $H_2$ and $C_2H_4$ gas are measured and admitted into $V_1 + V_2$ and allowed to thoroughly mix for ≥5 min. At time $t = 0$, the reactant gas mixture is allowed to contact the $Pd/Al_2O_3$ surface by opening valve $X_1$ while the pressure gauge output is recorded on a chart recorder.

For each experiment involving a different total initial pressure of $H_2 + C_2H_4$, a control experiment is made by allowing an identical initial pressure of $N_2(g)$ to expand into the catalyst cell. Likewise, the pressure drop with time is measured on the chart recorder. A typical result is shown in Figure 10, top panel. The control expansion of $N_2(g)$ at the same initial pressure as $C_2H_4(g) + H_2(g)$ is a convenient way to determine the pressure drop due to the change in volume upon opening the valve. In addition, it is assumed that the quantity of $N_2$ adsorbed is negligible and that the dynamics of the expansion in each case ($N_2$ vs. $C_2H_4 + H_2$) are very similar.

The bottom panel of Figure 10 shows how the difference between the $N_2$ expansion and the $C_2H_4 + H_2$ expansion, $\Delta P(t)$, can be plotted to give information about hydrogenation rates for

many different initial pressures of $H_2(g)$ and $C_2H_4(g)$. In the particular experiment shown, $P^\circ_{C_2H_4}$ was held constant while $P^\circ_{H_2}$ was varied in each experiment to determine the kinetic order with respect to $H_2$. The initial pressure decrease with time, $[\Delta P(t)]$, is usually linear, or very nearly so, in the first 3 to 4 s and is used as a measure of the initial rate of the hydrogenation reaction. Departures from linearity after ~5 s are due mainly to the consumption of reactants. We are confident that in the first few seconds of the reaction, diffusion of reactants through the gas phase to the catalyst surface is not a significant rate-controlling factor, based on control experiments which will be discussed shortly.

Data such as that in the bottom panel of Figure 10 can be treated by the following analysis of the linear least-squares derived initial slope. The stoichiometry of the reaction, 2 mol → 1 mol, makes the pressure a convenient method of monitoring the rate. The initial rate is given by eq 6, where $dN_{C_2H_6}/dt$ = molecules·s$^{-1}$,

$$\text{rate}_i = R_i = \left(\frac{dN_{C_2H_6}}{dt}\right)_i = -\frac{V_{Tot}\cdot N_A}{RT}\frac{dP_i}{dt} \qquad (6)$$

and $dP_i/dt$ = initial slope. The initial slope has units torr·s$^{-1}$; $V_{tot}$ = 299.2 cm$^3$; $N_A$ is Avogadro's number; $R$ = 6.236 × 10$^4$ cm$^3$·torr·mol$^{-1}$·K$^{-1}$; and $T$ is the temperature in Kelvin. The initial rate is then given in molecules·s$^{-1}$, with typical values in the $10^{16}$ to $10^{17}$ molecule·s$^{-1}$ range (~3.1 × 10$^{13}$ molecule·cm$^{-2}$·s$^{-1}$). Our conservative estimate of the precision by this technique is ±6%, with the largest contribution being due to our inability to precisely determine $\Delta P(t)$ in the region of steepest slope (see Figure 10).

We have conducted experiments to determine if our measured rates are being limited by the diffusion of reactants to the surface. By keeping the initial pressures of $H_2(g)$ and $C_2H_4(g)$ equal and constant at 0.0500 torr and increasing the initial pressure of $N_2$ which is added along with the $C_2H_4(g)$ + $H_2(g)$, the effect on the kinetics from diffusion of reactants through background $N_2(g)$ was checked. These data are shown in Figure 11. There is clearly no strong functional dependence of the measured initial rate on the total pressure at these pressures. Even for experiment 6, where 60% of the initial gas phase is composed of $N_2$, there is no apparent effect of diffusion through the $N_2(g)$ on the measured rate. This result, in conjunction with the fact that all rate measurements were made at $H_2$ + $C_2H_4$ total gas pressures ≤0.250 torr, is strong evidence that our measured rates are not being limited by diffusion of reactants through the gas phase to the catalyst surface.

# IR Transition Moment Directions in Matrix-Isolated Dimethylsilylene and 1-Methylsilene

**Gerhard Raabe,[1a,b] H. Vančik,[1a] Robert West,[1c] and Josef Michl*[1a]**

*Contribution from the Departments of Chemistry, University of Utah, Salt Lake City, Utah 84112, and University of Wisconsin—Madison, Madison, Wisconsin 53706.* *Received July 23, 1985*

**Abstract:** Irradiation of matrix-isolated dimethyldiazidosilane yields dimethylsilylene (**1**) as the major product. Photoselection on the 450-nm absorption band of **1** with polarized 488-nm light, which converts **1** into 1-methylsilene (**2**), permitted the assignment of six IR transitions of **1** and twelve IR transitions of **2** as in-plane or out-of-plane polarized. Photoselection on the 260-nm absorption band of **2** with polarized 248-nm light, which converts **2** back into **1**, allowed a determination of the absolute values of polarization angles of seven in-plane polarized IR transitions of **2** relative to the $\pi\pi^*$ transition moment. The resulting map of the IR transition moment directions in the molecule of **1** provides strong support for the detailed assignment of the nature of the vibrational motions involved. Along with other data, the results leave very little doubt as to the correctness of the structural and vibrational assignments in **1** and **2**.

Although Turner and collaborators[2] have demonstrated the power of the combined use of UV-visible photoselection and IR linear dichroism on molecules isolated in rare-gas matrices, the procedure has seen only limited further development. We now wish to report (i) its qualitative use to extend the symmetry assignments of the vibrations of dimethylsilylene (**1**) from two[3] to six fundamentals and (ii) its quantitative use to determine the polarization directions of twelve fundamental vibrations of 1-methylsilene (**2**), previously[3] only characterized as in-plane or out-of-plane polarized. To our knowledge, this is the first determination of IR polarization angles on a matrix-isolated molecule of low ($C_s$) symmetry.

The choice of **1** and **2** for targets of a detailed IR investigation was motivated in part by the still novel nature of the Si=C moiety, whose force field is of considerable interest.[3,4] In addition, it appears desirable to establish the identity and spectral properties of matrix-isolated **1** and **2** in an unassailable fashion in response to the recently raised doubts.[5,6] We have summarized the arguments in favor of the original assignments[3,7-9] elsewhere.[10] In our judgment, the evidence now is quite overwhelming.

The great improvement in the signal-to-noise ratio in the presently obtained dichroic spectra relative to prior work[3] was made possible by the use of dimethyldiazidosilane as a photochemical precursor[10] for **1**. The mechanism of the multistep

(1) (a) University of Utah. (b) Presented at the XIX Organosilicon Symposium, Louisiana State University, Baton Rouge, LA, April 26 and 27, 1985. (c) University of Wisconsin—Madison.

(2) E.g.: Burdett, J. K.; Grzybowski, J. M.; Perutz, R. N.; Poliakoff, M.; Turner, J. J.; Turner, R. F. *Inorg. Chem.* **1978**, *17*, 147. Church, S. P.; Poliakoff, M.; Timney, J. A.; Turner, J. J. *J. Am. Chem. Soc.* **1981**, *103*, 7515.

(3) Arrington, C. A.; Klingensmith, K. A.; West, R.; Michl, J. *J. Am. Chem. Soc.* **1984**, *106*, 525.

(4) Schlegel, H. B.; Wolfe, S.; Mislow, K. *J. Chem. Soc., Chem. Commun.* **1975**, 246. Baskir, E. G.; Maltsev, A. K.; Nefedov, O. M. *Izv. Akad. Nauk SSSR, Ser. Khim* **1983**, 1314. Maltsev, A. K.; Khabashesku, V. N.; Nefedov, O. M. *J. Organomet. Chem.* **1984**, *271*, 55.

(5) Hawari, J. A.; Griller, D. *Organometallics* **1984**, *3*, 1123.

(6) Nazran, A. S.; Hawari, J. A.; Griller, D.; Alnaimi, I. S.; Weber, W. P. *J. Am. Chem. Soc.* **1984**, *106*, 7267.

(7) Drahnak, T. J.; Michl, J.; West, R. *J. Am. Chem. Soc.* **1979**, *101*, 5427.

(8) Drahnak, T. J.; Michl, J.; West, R. *J. Am. Chem. Soc.* **1981**, *103*, 1845.

(9) Maier, G.; Mihm, G.; Reisenauer, H. P.; Littmann, D. *Chem. Ber.* **1984**, *117*, 2369.

(10) Vančik, H.; Raabe, G.; Michalczyk, M. J.; West, R.; Michl, J. *J. Am. Chem. Soc.* **1985**, *107*, 4097.

0002-7863/86/1508-0671$01.50/0 